On the non-convexity issue in the radial Calderón problem

Giovanni S. Alberti* Romain Petit† Clarice Poon‡ Irène Waldspurger§

November 24, 2025

Abstract

A classical approach to the Calderón problem is to estimate the unknown conductivity by solving a nonlinear least-squares problem. It leads to a nonconvex optimization problem which is generally believed to be riddled with bad local minimums. We revisit this issue in the case of piecewise constant radial conductivities and prove that, contrary to previous claims, there are no spurious critical points in the case of two scalar unknowns with no measurement noise. We also provide a partial proof of this result in the general setting which holds under a numerically verifiable assumption. Finally, we investigate whether a recently proposed approach based on convexification yields better reconstructions. For the first time, we propose a way to implement it in practice and show that it is consistently outperformed by some least squares solvers, which are also faster and require less measurements.

1 Introduction

1.1 Electrical impedance tomography and the Calderón problem

Electrical impedance tomography is a non-invasive imaging technique that consists in reconstructing the electrical conductivity of a medium from current-voltage boundary measurements. It was formalized in Calderón (1980) as an inverse problem for a partial differential equation (PDE), and is hence often called the *Calderón problem*. More precisely, the unknown of this inverse problem is modeled as a positive bounded function $\gamma : \Omega \to \mathbb{R}$ in a domain Ω. The application of an electrical current g on the boundary of the domain induces an electric potential u in Ω which is the unique solution to the following conductivity equation:

$$\begin{cases} \operatorname{div}(\gamma \nabla u) = 0 & \text{in } \Omega, \\ \gamma \partial_\nu u = g & \text{on } \partial\Omega. \end{cases}$$

The Calderón problem consists in recovering γ from the current-to-voltage map (also called Neumann-to-Dirichlet map) $\Lambda(\gamma) : g \mapsto u_{|\partial\Omega}$.

Although the map Λ can be shown to be injective (given sufficiently many measurements, see the references in the section below), it is highly ill-posed. As only boundary measurements are available, large variations of the unknown γ away from the boundary might result in very small variations of the measurements $\Lambda(\gamma)$. Coupled with the issue that the forward map Λ is nonlinear, the numerical resolution of the inverse problem is difficult, as reconstruction algorithms are potentially prone to the presence of local minimums and they might have to be carefully initialized. It is often mentioned that, due to the nonlinearity, the classical least squares approach leads to a nonconvex optimization problem which is riddled with bad local minimums. Some recent references where this claim was reiterated include Lazzaro et al. (2024); Brojatsch

*Machine Learning Genoa Center (MaLGa), Department of Mathematics, Department of Excellence 2023–2027, University of Genoa (giovanni.alberti@unige.it).

†CNRS and DMA, ENS, PSL Université (romain.petit@ens.fr).

‡Mathematics Institute, University of Warwick (clarice.poon@warwick.ac.uk).

§CNRS, Université Paris Dauphine, INRIA Mokaplan (waldspurger@ceremade.dauphine.fr).

and Harrach (2024); Klibanov et al. (2025); Harrach and Meftahi (2025). However, there is a lack of precise characterization in the literature on the nature of this non-convexity.

In this work, we revisit the non-convexity issue in the case of piecewise constant radial conductivities. We find that some least squares solvers always converge to a global minimizer. We provide a proof of the absence of spurious critical points in the case of two scalar unknowns. We also prove this result in the general case under a numerically verifiable assumption. In the absence of noise, our numerical simulations suggest that local minimums are not present and that the nonconvexity issue for the Calderón problem is far more nuanced than the literature suggests. Instead, the real challenge seems to be the ill-posedness of the inverse problem. Motivated by these findings, we also investigate whether the recently proposed convexification approach of Harrach (2023) can still lead to improved reconstructions. We propose a way to implement it in practice and conduct an extensive numerical comparison with the least squares approach, showing that the former is consistently outperformed by the latter.

1.2 Previous works

Theoretical study of the Calderón problem. The landmark results of Sylvester and Uhlmann (1987); Nachman (1996) (see also the later works Astala and Päivärinta (2006); Bukhgeim (2008); Caro and Rogers (2016)) show that, under suitable assumptions, the unknown conductivity γ is entirely determined by the Neumann-to-Dirichlet map $\Lambda(\gamma)$. We stress that this amounts to assume that one has access to infinitely many measurements. More recently, identifiability from finitely many measurements has been investigated in Alberti and Santacesaria (2019, 2022). Regarding robustness to measurement noise, the ill-posedness of the problem only allows for weak stability results (Alessandrini, 1988; Mandache, 2001), unless some strong a priori information on the unknown is available (Alessandrini and Vessella, 2005; Bacchelli and Vessella, 2006; Beretta et al., 2013; Beretta and Francini, 2022).

Reconstruction methods. The most common approach to solve the Calderón problem is to rely on Landweber iteration, which amounts to performing gradient descent on a nonlinear least squares objective. As this objective is non-convex, convergence to a global minimizer is not guaranteed. Many works have been devoted to the introduction of conditions under which local convergence can be proved (see for example Hanke et al. (1995); Neubauer (2000); Kaltenbacher et al. (2008)). Whether these conditions are satisfied in the context of the Calderón problem is, to our knowledge, an open question (see Lechleiter and Rieder (2008); Kindermann (2022); Kaltenbacher (2024) for some partial results). In this setting, global convergence seems very difficult to prove. Another class of reconstruction techniques are direct methods Nachman (1996); Siltanen et al. (2000), which however are not considered in this work.

Convex programming approaches. In Harrach (2023), it is proved that, when the number of measurements is sufficiently large, the sought-after conductivity is the unique solution of a convex program which depends on the unknown only through the measurements. This property is particularly interesting, since convex optimization problems can be solved with globally convergent algorithms (that is to say, whose convergence is guaranteed for every choice of initial point). To our knowledge, this is the first convexification result that is valid in the finite measurements and noisy setting. However, the proof of this result is not constructive, and no procedure to find the minimal number of measurements is proposed. In addition, the property only holds under strong conditions on the parameters defining the convex program. How to find admissible values for these parameters in practice is not discussed. As a result, this reconstruction method has not been implemented and numerically compared with existing approaches. Let us also mention that other convexification methods based on Carleman estimates have been proposed in Klibanov et al. (2017, 2019) in the case of infinitely many measurements and diminishing noise. Finally, a convex approach based on lifting is discussed in Alberti et al. (2025).

Radial conductivities. Numerous works were dedicated to the special setting of radial conductivities (see for instance Sylvester (1992); Knudsen et al. (2007); Barceló et al. (2024); Daudé et al. (2024)). In Siltanen

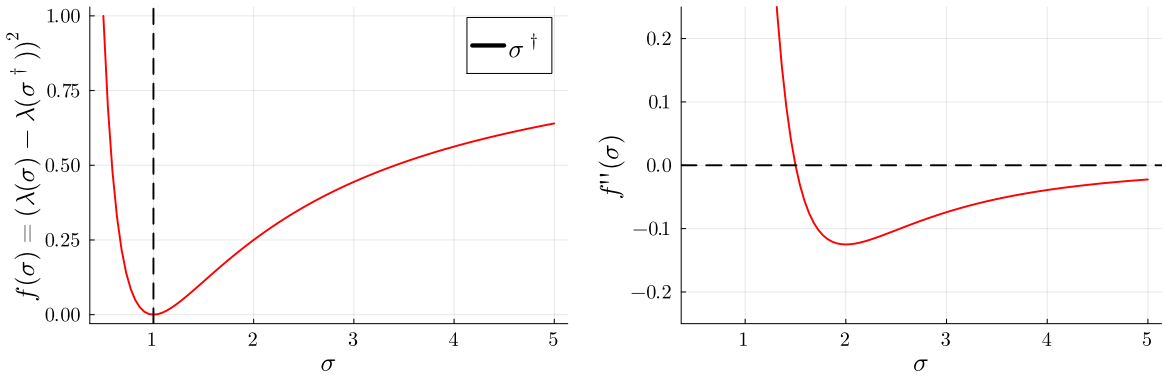

(a) (b)

Figure 1: plot of the least squares objective (a) and its second derivative (b) in a one-dimensional setting. The objective is not convex (its second derivative is not nonnegative), but it has a single critical point, which is its global minimum.

et al. (2000), the explicit expression of the forward map for radial *and* piecewise constant conductivities is computed. Assuming infinitely measurements are available, Garde (2020, 2022) develops a reconstruction algorithm based on a series of one-dimensional optimization problems for a particular class of piecewise constant conductivities, which covers the radial setting. To our knowledge, the only work studying the optimization landscape of least squares in this setting is Harrach (2023, Section 2).

1.3 Contributions

We focus on the simple setting of piecewise constant radial conductivities, which allows us to obtain a finite-dimensional inverse problem. We prove two new properties in the case of conductivities that are defined by two scalar unknowns. We show that they are uniquely determined by two scalar measurements, and that the corresponding least squares objective in the noiseless case has no spurious critical points. We also prove that these results can be extended to the higher dimensional case under a numerically verifiable assumption. We visualize these facts in the simpler setting with a one-dimensional unknown and one scalar measurement in Figure 1: despite the non-convexity, the squared loss has a single critical point, corresponding to the true unknown, and there are no local minima.

Concerning the convex reformulation of the Caderón problem introduced in Harrach (2023), we propose a numerical procedure to evaluate this formulation. We first introduce a method to estimate the parameters of the convex program by exploiting its optimality conditions. We then show that the convex program can be solved efficiently with interior point algorithms. We extensively compare this approach with the classical least squares approach. We provide an open source Julia package called `RadialCalderon.jl`[1] which allows one to reproduce all our experiments (see Bezanson et al. (2017) for more background on the Julia language). This package can be used to benchmark different reconstruction methods and study numerically this radial piecewise constant version of the Calderón problem.

Our results suggest that the convex programming approach only allows for an accurate estimation of the unknown for problems with a very small size. It is consistently outperformed by the least squares approach, which is faster and more accurate while requiring less measurements. We argue that circumventing the nonconvexity of the problem without addressing its ill-posedness cannot yield an accurate estimation procedure.

[1] https://github.com/rpetit/RadialCalderon.jl (see also https://rpetit.github.io/RadialCalderon.jl for tutorials and the full documentation).

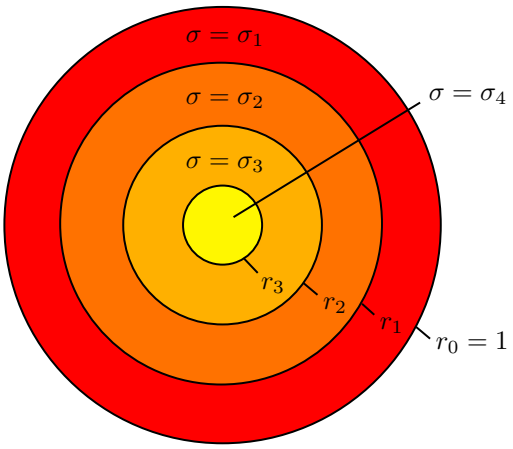

Figure 2: schematic description of the piecewise constant radial setting when $n = 4$. The conductivity $\gamma : B(0,1) \to \mathbb{R}$ is such that, using the polar coordinates (r, θ), it holds $\gamma(r, \theta) = \sigma_i$ for every $r_i < r < r_{i-1}$ for some $\sigma = (\sigma_i)_{1 \leq i \leq n} \in (\mathbb{R}_{>0})^n$.

Plan of the paper. In Section 2, we introduce the setting of piecewise constant radial conductivities. In Section 3, we analyze the case of conductivities that are defined by two scalar unknowns, and discuss the extension of our results to the higher dimensional setting. In Section 4, we introduce the resolution method proposed in Harrach (2023) and propose a method for estimating all the parameters of the related convex program. In Section 5, we perform an extensive numerical comparison of this method with the least squares approach. Finally, some concluding remarks are discussed in Section 6.

2 Piecewise constant radial conductivities

In this section, we introduce the setting of radial piecewise constant conductivities, which has all the important features of the full Calderón problem. Its main interest is to allow the evaluation of the forward map without having to rely on finite element methods to solve the underlying PDE. This allows us to decouple the study of the inverse problem and its ill-posedness from the effect of numerical errors in the evaluation of the forward map.

2.1 Setting

We work on the two-dimensional open unit ball $\Omega = B(0,1)$ and assume that the unknown conductivity is piecewise constant on a known partition of Ω made of concentric annuli. More precisely, we use the polar coordinates (r, θ) and assume that $\gamma(r, \theta)$ is equal to a positive constant $\sigma_i > 0$ for every $r_i < r < r_{i-1}$ with $0 = r_n < r_{n-1} < ... < r_0 = 1$ (see Figure 2 for a schematic description). For every vector $\sigma \in (\mathbb{R}_{>0})^n$, we denote by γ_σ the associated function, where $\mathbb{R}_{>0}$ denotes the set of positive real numbers.

As noticed in Siltanen et al. (2000, Lemma 4.1), taking the Neumann data to be cosine functions allows us to obtain a diagonal Neumann-to-Dirichlet map. To be more precise, we fix a number of scalar measurements m, and, given $j \in \{1, ..., m\}$, we define $g_j : \partial\Omega \to \mathbb{R}$ by $g_j(\theta) = \cos(j\theta)$. We notice as in Siltanen et al. (2000, Lemma 4.1) that if $u_j(r, \theta) = (\alpha_{i,j} r^j + \beta_{i,j} r^{-j}) \cos(j\theta)$ for every $r_i < r < r_{i-1}$ then u_j is a solution to the Neumann problem for the conductivity equation

$$\begin{cases} \operatorname{div}(\gamma_\sigma \nabla u_j) = 0 & \text{in } \Omega, \\ \gamma_\sigma \partial_\nu u_j = g_j & \text{on } \partial\Omega, \end{cases}$$

provided $\beta_{n,j} = 0$, $\sigma_1 j(\alpha_{1,j} - \beta_{1,j}) = 1$ and

$$\begin{cases} \alpha_{i,j} r_i^j + \beta_{i,j} r_i^{-j} = \alpha_{i+1,j} r_i^j + \beta_{i+1,j} r_i^{-j}, \\ \sigma_i(\alpha_{i,j} r_i^j - \beta_{i,j} r_i^{-j}) = \sigma_{i+1}(\alpha_{i+1,j} r_i^j - \beta_{i+1,j} r_i^{-j}), \end{cases} \tag{1}$$

for every $1 \leq i \leq n-1$ and $1 \leq j \leq m$. It is shown in Siltanen et al. (2000, Lemma 4.1) that the solution of (1) satisfies $\beta_{i,j} = C_{i,j}\alpha_{i,j}$ with

$$C_{n,j} = 0 \quad \text{and} \quad C_{i,j} = \frac{\rho_i r_i^{2j} + C_{i+1,j}}{1 + \rho_i C_{i+1,j} r_i^{-2j}}, \tag{2}$$

where $\rho_i \overset{\text{def.}}{=} (\sigma_i - \sigma_{i+1})/(\sigma_i + \sigma_{i+1})$.

Since $u_{j\,|\partial\Omega} = (\alpha_{1,j} + \beta_{1,j})\cos(j\theta)$, we obtain that the Neumann-to-Dirichlet map introduced in Section 1.1 satisfies $\Lambda(\gamma_\sigma) g_j = \lambda_j(\sigma) g_j$ with

$$\lambda_j(\sigma) \overset{\text{def.}}{=} \frac{1 + C_{1,j}}{j\sigma_1(1 - C_{1,j})}. \tag{3}$$

Finite-dimensional forward map. Abusing notation, we also denote by Λ the following truncated Neumann-to-Dirichlet map:

$$\begin{aligned} \Lambda \colon (\mathbb{R}_{>0})^n &\to \mathbb{R}^m \\ \sigma &\mapsto [\lambda_j(\sigma)]_{j=1}^m. \end{aligned}$$

In the following, we focus on the recovery of σ from the knowledge of $\Lambda(\sigma)$, which is an inverse problem with a finite-dimensional unknown and finitely many measurements.

In practice, the forward map Λ can be evaluated by computing $C_{1,j}$ using (2) and plugging the result in the expression of $\lambda_j(\sigma)$. The Jacobian and the Hessian of Λ can also be computed efficiently via automatic differentiation. To compute them, we use the package `ForwarDiff.jl` (Revels et al., 2016) via `DifferentiationInterface.jl` (Dalle and Hill, 2024; Hill and Dalle, 2025; Schäfer et al., 2022).

The following proposition gives some properties of the forward map Λ, on which we crucially rely.

Proposition 2.1 *The mapping Λ is convex. In addition, it is strictly decreasing, meaning that for every $\sigma, \sigma' \in (\mathbb{R}_{>0})^n$ with $\sigma \leq \sigma'$ (pointwise) and $\sigma \neq \sigma'$, it holds $\lambda_j(\sigma) > \lambda_j(\sigma')$ for every $1 \leq j \leq m$.*

Proof. The convexity of Λ is proved in Harrach (2023, Lemma 4.1). From the same reference, we have that the partial derivative of λ_j with respect to its i-th variable (that is σ_i) satisfies

$$\partial_i \lambda_j(\sigma) = -\frac{1}{\pi} \int_{A_i} \|\nabla u_j(\tau)\|_2^2 d\tau, \tag{4}$$

where A_i denotes the annulus $r_i < r < r_{i-1}$. We claim that this quantity is negative for every $1 \leq i \leq n$ and $1 \leq j \leq m$. To see this, we notice that, since γ_σ is lower bounded by the positive constant $\min_{1 \leq i \leq n} \sigma_i$, the differential operator $\operatorname{div}(\gamma_\sigma \nabla \cdot)$ is uniformly elliptic. As a result, the strong unique continuation principle (see for instance Alessandrini (2012)) ensures that, if u_j vanishes on a non empty open set, it is identically zero. Since the boundary data g_j is not identically zero, we obtain that u_j is not identically zero. If u_j was equal to a constant on a non empty open set, the same argument could be applied to u_j minus this constant, which still solves $\operatorname{div}(\gamma_\sigma \nabla u_j) = 0$. As a result, we obtain that ∇u_j cannot vanish on a non empty open set, which yields the result. □

2.2 Numerical study of the inverse problem

In this section, we present several experiments suggesting that this simple piecewise constant radial model exhibits all the important features of the classical Calderón problem. In particular, the estimation problem becomes increasingly ill-posed away from the boundary. In the following, we take $r_i = (n-i)/n$ $(i = 0, ..., n)$.

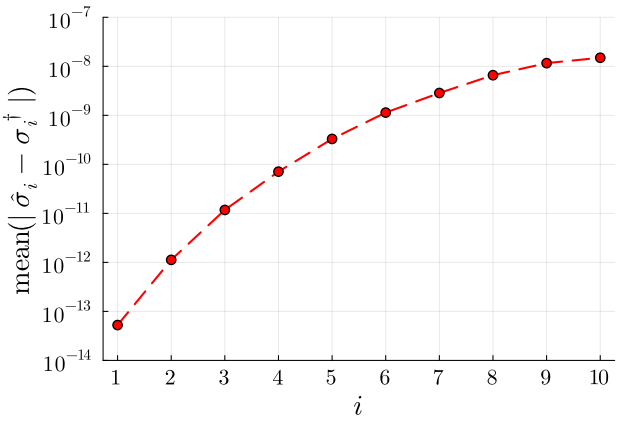

Figure 3: mean error on the i-th annulus among 100 pairs $\sigma^\dagger, \hat{\sigma} \in [a,b]^n$ such that $\|\Lambda(\hat{\sigma}) - \Lambda(\sigma^\dagger)\|_\infty \leq 10^{-15}$ with $(a,b) = (0.5, 1.5)$ and $n = m = 10$. The error on the outermost annulus is several orders of magnitude smaller than the error on the innermost annulus.

Our first experiment shows that the estimation of the conductivity is much harder on annuli that are distant from the boundary. We take $n = m = 10$ and draw 100 random true conductivities uniformly in $[a,b]^n$ with $a = 0.5$ and $b = 1.5$. Then, we use a trust-region algorithm to solve the nonlinear equation $\Lambda(\sigma) = \Lambda(\sigma^\dagger)$ for each true conductivity $\sigma^\dagger$. For each instance, we require that the estimated conductivity $\hat{\sigma}$ satisfies $\|\Lambda(\hat{\sigma}) - \Lambda(\sigma^\dagger)\|_\infty \leq 10^{-15}$, where $\|\cdot\|_\infty$ denotes the euclidean ℓ^∞ norm (the maximum of the absolute values of the coordinates). Then, we compute the mean of $|\hat{\sigma}_i - \sigma_i^\dagger|$ for each $i \in \{1, ..., n\}$. The result is given in Figure 3. We notice that the average error increases by several orders of magnitude as i grows. This is consistent with the well-known fact that the reconstruction quality deteriorates as one moves away from the boundary, see e.g. Winkler and Rieder (2014); Garde and Knudsen (2017); Alessandrini and Scapin (2017); Garde and Hyvönen (2020). Taking m much larger than n yields similar results.

Our second experiment shows that the inverse problem becomes more and more ill-posed as n grows, as expected given the severe ill-posedness of the infinite-dimensional inverse problem, see Rondi (2006). Indeed, given $\epsilon > 0$, we notice that the quantity

$$\sup_{\sigma,\sigma' \in [a,b]^n} \|\sigma - \sigma'\|_\infty \quad \text{s.t.} \quad \|\Lambda(\sigma) - \Lambda(\sigma')\|_\infty \leq \epsilon$$

significantly increases as n increases. To show this, we run the same experiment as above with $n = m$ ranging from 2 to 10. The results are displayed in Figure 4. Again, taking m much larger than n yields similar results.

Finally, we notice that $\Lambda'(\sigma)$ (the Jacobian matrix of Λ at σ) seems to be always invertible when $m = n$, but that its smallest singular value goes to 0 as n increases (see Table 1 in Section 3). When $m > n$, there are always n nonzero singular values.

3 Identifiability and absence of bad critical points

We prove in this section that, when $n = 2$ and $m \geq 2$, the forward map Λ is injective. We also show that, when $n = 2$ and $m \geq n$, for every $\sigma^\dagger \in (\mathbb{R}_{>0})^n$, the least squares objective $\sigma \mapsto \|\Lambda(\sigma) - \Lambda(\sigma^\dagger)\|_2^2$ has a unique critical point, which is $\sigma^\dagger$. Finally, we provide a discussion concerning the case where $n > 2$. Our results suggest that, in this piecewise constant radial setting, the main difficulty for solving the inverse problem is not the nonconvexity of the least squares objective, but rather the ill-posedness of the problem.

Throughout, given $\Lambda : \sigma \in (\mathbb{R}_{>0})^n \to (\lambda_i(\sigma))_{i=1}^m$, its Jacobian is denoted by $\Lambda'(\sigma) \in \mathbb{R}^{m \times n}$ with its (j,i)-th entry in row j and column i being $\partial_i \lambda_j(\sigma)$.

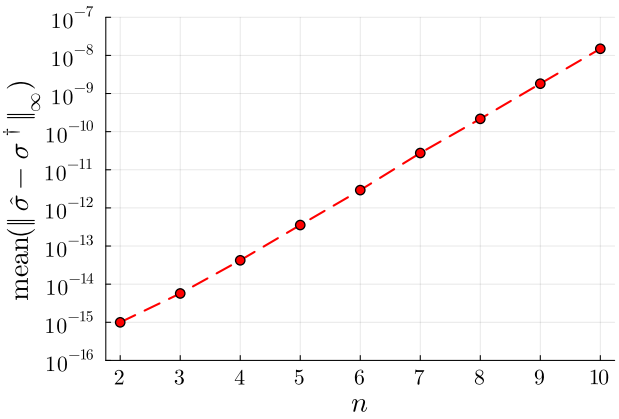

Figure 4: mean ℓ^∞ error as a function of the number of annuli n. The mean is computed on 100 pairs $\sigma^\dagger, \hat{\sigma} \in [a,b]^n$ such that $\|\Lambda(\hat{\sigma}) - \Lambda(\sigma^\dagger)\|_\infty \leq 10^{-15}$ with $(a,b) = (0.5, 1.5)$ and $m = n$ measurements.

3.1 The two-dimensional case

In the particular case of two scalar unknowns ($n = 2$), (2) and (3) yield

$$\lambda_j(\sigma) = \frac{1 + \rho_1 r_1^{2j}}{j\sigma_1(1 - \rho_1 r_1^{2j})} \tag{5}$$

for every $1 \leq j \leq m$.

We first state the following useful lemma.

Lemma 3.1 *Let $n = m = 2$ and consider $\Lambda : \sigma \mapsto (\lambda_1(\sigma), \lambda_2(\sigma))$. Then, the determinant of the Jacobian is negative, that is to say $\det(\Lambda'(\sigma)) < 0$ for all $\sigma \in (\mathbb{R}_{>0})^2$.*

Proof. As shown in the proof of Proposition 2.1, we have $\partial_i \lambda_j(\sigma) < 0$. Let

$$h_j(\sigma) \overset{\text{def.}}{=} \frac{\partial_1 \lambda_j(\sigma)}{\partial_2 \lambda_j(\sigma)}.$$

Then, one can check (we obtained this expression by relying on a symbolic computation tool) that for every $\sigma = (\sigma_1, \sigma_2) \in (\mathbb{R}_{>0})^2$, it holds

$$h_j(\sigma) = \frac{1}{4\sigma_1^2}\left(\frac{1}{r_1^{2j}}(\sigma_1 + \sigma_2)^2 - r_1^{2j}(\sigma_1 - \sigma_2)^2 - 4\sigma_1\sigma_2\right), \tag{6}$$

which is clearly increasing in j, since $r_1 \in (0,1)$ implies that each of the terms is increasing in j. It follows that

$$\det(\Lambda'(\sigma)) = \partial_1\lambda_1(\sigma)\partial_2\lambda_2(\sigma) - \partial_1\lambda_2(\sigma)\partial_2\lambda_1(\sigma) = \partial_2\lambda_2(\sigma)\partial_2\lambda_1(\sigma)[h_1(\sigma) - h_2(\sigma)] < 0,$$

where we have used also that $\partial_i\lambda_1(\sigma) < 0$ ($i = 1, 2$). □

Now, we prove that the unknown conductivity can be recovered from two scalar measurements. To our knowledge, the best identifiability results that are currently available require a number of measurements which is exponential in the number of unknowns (Alberti and Santacesaria, 2022).

Proposition 3.2 *If $n = 2$ and $m \geq 2$, the forward map Λ is injective.*

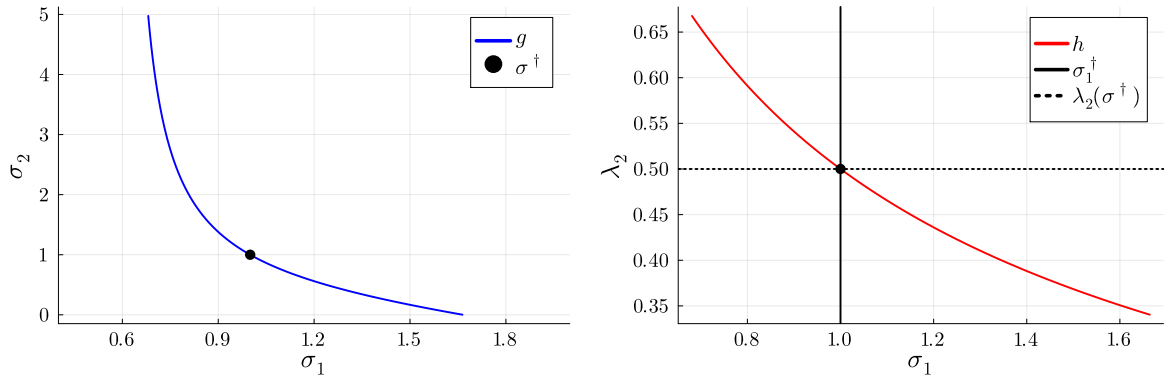

(a) (b)

Figure 5: graph of the functions g and h constructed in the proof of Proposition 3.2, with $\sigma^\dagger = \mathbf{1}$. The function h is strictly monotone, showing that the forward map is injective.

Proof. It is enough to prove the result in the case $m = 2$. Let $\sigma^\dagger, \hat{\sigma} \in (\mathbb{R}_{>0})^2$ be such that $\sigma^\dagger \neq \hat{\sigma}$ and $\Lambda(\sigma^\dagger) = \Lambda(\hat{\sigma})$. By strict monotonicity (Proposition 2.1), we can assume without loss of generality that $\sigma_1^\dagger < \hat{\sigma}_1$ and $\sigma_2^\dagger > \hat{\sigma}_2$.

We first show that there exists a function $g : [\sigma_1^\dagger, \hat{\sigma}_1] \to [\hat{\sigma}_2, \sigma_2^\dagger]$ such that $\lambda_1(\sigma_1, g(\sigma_1)) = \lambda_1(\sigma^\dagger)$ for every $\sigma_1 \in [\sigma_1^\dagger, \hat{\sigma}_1]$. For visualization purposes, the graph of this function, as well as the graph of the function h that we compute below, is given in Figure 5 in the case where $\sigma^\dagger = \mathbf{1}$. Define $f(\sigma) = \lambda_1(\sigma) - \lambda_1(\sigma^\dagger)$. Then, by monotonicity,

- f is negative on $(\sigma_1^\dagger, \hat{\sigma}_1) \times \{\sigma_2^\dagger\}$,
- f is positive on $(\sigma_1^\dagger, \hat{\sigma}_1) \times \{\hat{\sigma}_2\}$.

It follows by the intermediate value theorem that for all $\sigma_1 \in (\sigma_1^\dagger, \hat{\sigma}_1)$, there exists $\sigma_2 \in (\hat{\sigma}_2, \sigma_2^\dagger)$ such that $f(\sigma_1, \sigma_2) = 0$. This shows that g is well defined. Moreover, since $\partial_2 \lambda_1 < 0$, it follows by the implicit function theorem that g is of class C^1 and $g'(\sigma_1) = -\partial_1 \lambda_1(\sigma, g(\sigma_1))/\partial_2 \lambda_1(\sigma_1, g(\sigma_1))$.

Now consider $h(\sigma_1) = \lambda_2(\sigma_1, g(\sigma_1))$. Since $g(\sigma_1^\dagger) = \sigma_2^\dagger$ and $g(\hat{\sigma}_1) = \hat{\sigma}_2$, by assumption, $h(\sigma_1^\dagger) = h(\hat{\sigma}_1)$. Observe also that

$$h'(\sigma_1) = \partial_1 \lambda_2(\sigma_1, g(\sigma_1)) + \partial_2 \lambda_2(\sigma_1, g(\sigma_1)) g'(\sigma_1) = \frac{(\partial_1 \lambda_2 \partial_2 \lambda_1 - \partial_1 \lambda_1 \partial_2 \lambda_2)}{\partial_2 \lambda_1},$$

where each term on the right-hand side is evaluated at $(\sigma_1, g(\sigma_1))$. We have $h'(\sigma_1) > 0$ for every $\sigma_1 \in (\sigma_1^\dagger, \hat{\sigma}_1)$ by Lemma 3.1, which contradicts the assumption that h takes the same value on two distinct points. □

Finally, we prove that, when $n = 2$ and $m \geq 2$, the least squares objective does not have any spurious critical point.

Proposition 3.3 *If $n = 2$ and $m \geq 2$, for every $\sigma^\dagger \in (\mathbb{R}_{>0})^n$, the least squares objective*

$$f : \sigma \mapsto \frac{1}{2} \|\Lambda(\sigma) - \Lambda(\sigma^\dagger)\|_2^2$$

has a unique critical point on $(\mathbb{R}_{>0})^n$, which is $\sigma^\dagger$.

Proof. First, let us stress that the result for $m = 2$ follows directly from Proposition 3.1. Indeed, if σ is a critical point then $\nabla f(\sigma) = [\Lambda'(\sigma)]^T(\Lambda(\sigma) - \Lambda(\sigma^\dagger)) = 0$. Since $[\Lambda'(\sigma)]^T \in \mathbb{R}^{2\times 2}$ is injective (by Proposition 3.1), this implies $\Lambda(\sigma) - \Lambda(\sigma^\dagger) = 0$. By injectivity of Λ (Proposition 3.2), we obtain $\sigma = \sigma^\dagger$. This argument does not carry on to the general case, as $[\Lambda'(\sigma)]^T \in \mathbb{R}^{2\times m}$ cannot be full rank when $m > 2$.

For the general case ($m \geq 2$), we define

$$\Phi\colon (\mathbb{R}_{>0})^2 \to \mathbb{R}_{>0}\times(-1,1) \qquad \mu_j\colon \mathbb{R}_{>0}\times(-1,1)\to\mathbb{R}$$
$$(\sigma_1,\sigma_2)\mapsto \left(\frac{1}{\sigma_1}, \frac{\sigma_1-\sigma_2}{\sigma_1+\sigma_2}\right) \quad \text{and} \quad (x,y)\mapsto \frac{x}{j}\frac{1+r_1^{2j}y}{1-r_1^{2j}y}$$

as well as $(x^\dagger, y^\dagger) = \Phi(\sigma^\dagger)$ and $g : (x,y) \in \mathbb{R}_{>0}\times(-1,1) \to (1/2)\sum_{j=1}^m(\mu_j(x,y) - \mu_j(x^\dagger,y^\dagger))^2$. As $f = g\circ\Phi$ and Φ is a diffeomorphism, a point σ is a critical point of f if and only if $\Phi(\sigma)$ is a critical point of g. Therefore, we only have to prove that $(x^\dagger, y^\dagger)$ is the only critical point of g.

Let $(x,y) \in \mathbb{R}_{>0}\times(-1,1)$ be fixed. We will show that, if $(x,y) \neq (x^\dagger,y^\dagger)$, then (x,y) is not a critical point of g. Let us first assume that

$$(x-x^\dagger)\left(x\frac{1+y}{1-y} - x^\dagger\frac{1+y^\dagger}{1-y^\dagger}\right) < 0. \tag{7}$$

Let R be the unique real number in $(0,1)$ such that

$$x\frac{1+Ry}{1-Ry} = x^\dagger\frac{1+Ry^\dagger}{1-Ry^\dagger}$$

which exists and is unique by (7). Then, for every $r \in \mathbb{R}$, it holds (from the factorization rules for degree two polynomials)

$$x\frac{1+ry}{1-ry} - x^\dagger\frac{1+ry^\dagger}{1-ry^\dagger} = \frac{x^\dagger - x}{(1-ry)(1-ry^\dagger)}(r-R)(yy^\dagger r + 1/R).$$

As a result, for every $1 \leq j \leq m$, it holds

$$\mu_j(x,y) - \mu_j(x^\dagger,y^\dagger) = \frac{1}{j}\frac{x^\dagger - x}{(1-r_1^{2j}y)(1-r_1^{2j}y^\dagger)}(r_1^{2j}-R)(yy^\dagger r_1^{2j} + 1/R).$$

For every $1 \leq j \leq m$ and $(\alpha,\beta) \in \mathbb{R}^2$, it holds

$$d\mu_j(x,y)\cdot(\alpha,\beta) = \frac{1}{j(1-r_1^{2j}y)}\left[\alpha(1+r_1^{2j}y) + \frac{2r_1^{2j}\beta x}{1-r_1^{2j}y}\right].$$

We evaluate this expression at $\alpha = -2Rx/(1-Ry)$ and $\beta = 1+Ry$ and obtain

$$\begin{aligned} d\mu_j(x,y)\cdot(\alpha,\beta) &= \frac{1}{j(1-r_1^{2j}y)}\left[-\frac{2R(1+r_1^{2j}y)x}{1-Ry} + \frac{2r_1^{2j}(1+Ry)x}{1-r_1^{2j}y}\right] \\ &= \frac{2x}{j(1-r_1^{2j}y)^2(1-Ry)}(r_1^{2j}-R)(1+Rr_1^{2j}y^2). \end{aligned}$$

Now, it holds that

$$\begin{aligned} dg(x,y)\cdot(\alpha,\beta) &= \sum_{j=1}^m(\mu_j(x,y)-\mu_j(x^\dagger,y^\dagger))d\mu_j(x,y)\cdot(\alpha,\beta) \\ &= \sum_{j=1}^m \frac{1}{j^2}\frac{2x(x^\dagger-x)}{(1-r_1^{2j}y)^3(1-r_1^{2j}y^\dagger)(1-Ry)}(r_1^{2j}-R)^2(yy^\dagger r_1^{2j}+1/R)(1+Rr_1^{2j}y^2). \end{aligned}$$

All terms inside the sum have the same sign as $x^\dagger - x$. Indeed $2x$, $1 - r_1^{2j} y$, $1 - r_1^{2j} y^\dagger$, $1 - Ry$ and $1 + R r_2^{2j} y^2$ are all positive and $y y^\dagger r_1^{2j} + 1/R \geq -|y||y^\dagger| r_1^{2j} + 1/R > -1 + 1/R > 0$ (since $R \in (0,1)$). The terms in the sum can only be zero if $r_1^{2j} = R$, which occurs for at most one value of j. Therefore, we have a sum of real numbers which have the same sign and are not all zero, meaning that $dg(x,y) \cdot (\alpha, \beta) \neq 0$ and (x,y) is not a critical point.

Now, we consider the case where (7) does not hold. This case is easier, as one can show that the sign of

$$r \in [0,1] \mapsto x \frac{1+ry}{1-ry} - x^\dagger \frac{1+ry^\dagger}{1-ry^\dagger}$$

does not change. Indeed, the fact that (7) does not hold means that this map has the same sign at 0 and 1. If $y y^\dagger \leq 0$, it is a monotonic function, so it cannot change sign over $[0,1]$. If $y y^\dagger > 0$, one can check by an explicit computation that it has two zeros, with opposite signs, so that it cannot cancel more than once in $(0,1)$. If it has the same sign at 0 and 1, it therefore does not cancel in $(0,1)$ at all, and the sign does not change over the interval.

Hence $\mu_j(x,y) - \mu_j(x^\dagger, y^\dagger)$ has the same sign for all values of j. Therefore, we have that

$$dg(x,y) \cdot (1,0) = \sum_{j=1}^{m} (\mu_j(x,y) - \mu_j(x^\dagger, y^\dagger)) \frac{1 + r_1^{2j} y}{j(1 - r_1^{2j} y)}$$

is a sum of terms with the same sign. Unless $\mu_j(x,y) = \mu_j(x^\dagger, y^\dagger)$ for every $1 \leq j \leq m$ (which is possible only if $(x,y) = (x^\dagger, y^\dagger)$), not all terms are zero, hence the sum is also non-zero and (x,y) is not a critical point. □

3.2 The higher dimensional case

In this section, we discuss the extension of the above results to the case $n > 2$. We restrict ourselves to the case $m = n$. Given $\sigma \in (\mathbb{R}_{>0})^n$, we denote by $\Lambda'_{[n-1]}(\sigma) \in \mathbb{R}^{(n-1)\times(n-1)}$ the submatrix of $\Lambda'(\sigma) \in \mathbb{R}^{n \times n}$ obtained by removing its last row (corresponding to the last measurement) and its first column (corresponding to the outermost annulus).

3.2.1 Main result

Our main result shows that, provided the following two conditions hold, the least squares objective has a unique critical point, which is the unknown conductivity. We discuss these conditions in greater details at the end of this section.

(i) Jacobian invertibility: for every $n \geq 2$ and every $\sigma \in (\mathbb{R}_{>0})^n$, $\Lambda'(\sigma)$ and $\Lambda'_{[n-1]}(\sigma)$ are invertible.

(ii) Alternating signs: for every $n \geq 2$, if $\sigma^\dagger, \hat{\sigma} \in (\mathbb{R}_{>0})^n$ are such that $\sigma_1^\dagger < \hat{\sigma}_1$ and $\lambda_j(\sigma^\dagger) = \lambda_j(\hat{\sigma})$ for every $j = 1, \ldots, n-1$, then $\operatorname{sign}(\sigma_i^\dagger - \hat{\sigma}_i) = (-1)^i$ for every $2 \leq i \leq n$, that is to say $\sigma_2^\dagger > \hat{\sigma}_2^\dagger$, $\sigma_3^\dagger < \hat{\sigma}_3^\dagger$, and so on.

Proposition 3.4 *Assume that conditions (i) and (ii) hold. Then, for every $n \geq 2$ and $m = n$, the least squares objective $f : \sigma \mapsto (1/2)\|\Lambda(\sigma) - \Lambda(\sigma^\dagger)\|_2^2$ has $\sigma^\dagger$ as its unique critical point in $(\mathbb{R}_{>0})^n$.*

Proof. Just as in the $n = 2$ setting, since condition (i) guarantees that $\Lambda'(\sigma)$ is invertible, it is sufficient to show that Λ is injective. We prove the injectivity by induction on n. For $n = 2$, this follows by Proposition 3.2. Assume now that the result is true for $n - 1$. Suppose by contradiction that there exist distinct $\sigma^\dagger$ and $\hat{\sigma}$ such that $\Lambda(\sigma^\dagger) = \Lambda(\hat{\sigma})$. Note that $\sigma_i^\dagger \neq \hat{\sigma}_i$ for all i, otherwise, this contradicts our induction assumption on the injectivity of Λ. Without loss of generality, we assume that $\hat{\sigma}_1 > \sigma_1^\dagger$. By the alternating signs condition (ii), we have $\sigma_2^\dagger > \hat{\sigma}_2^\dagger$, $\sigma_3^\dagger < \hat{\sigma}_3^\dagger$, and so on.

Let $I \overset{\text{def.}}{=} [\sigma_1^\dagger, \hat{\sigma}_1]$. We first claim that for all $\sigma_1 \in I$, there exists a differentiable function $g\colon I \to (\mathbb{R}_{>0})^{n-1}$ such that

$$\forall j = 1, \dots, n-1, \quad \lambda_j(\sigma_1, g(\sigma_1)) = \lambda_j(\sigma^\dagger).$$

Certainly, any such g satisfies $g(\sigma_1^\dagger) = (\sigma_i^\dagger)_{i=2}^{n-1}$ and $g(\hat{\sigma}_1) = (\hat{\sigma}_i)_{i=2}^{n-1}$. Note also that by the implicit function theorem, any such g has differential

$$g'(\sigma_1) = -(\Lambda'_{[n-1]})^{-1} \left(\partial_1 \lambda_j\right)_{j=1}^{n-1}, \tag{8}$$

where, as a slight abuse of notation, we write $\Lambda'_{[n-1]} \overset{\text{def.}}{=} \Lambda'_{[n-1]}(\sigma_1, g(\sigma_1))$. Note that, by assumption (i), $\Lambda'_{[n-1]}$ is invertible.

We now claim that g is well defined on I and maps into the cuboid

$$B = [\hat{\sigma}_2, \sigma_2^\dagger] \times [\sigma_3^\dagger, \hat{\sigma}_3] \times [\hat{\sigma}_4, \sigma_4^\dagger] \times \cdots.$$

Indeed, since $C = \{\sigma \in (\mathbb{R}_{>0})^n : \ \forall j = 1, \dots, n-1, \ \lambda_j(\sigma) = \lambda_j(\sigma^\dagger)\}$ is a closed set, the only reason why g might not exist on I is that $g(\sigma_1)_i$ diverges to infinity or converges to 0. This cannot happen because we can apply the implicit function theorem at $\hat{\sigma}$ (and $\sigma^\dagger$) to conclude that g exists on a neighborhood around $\hat{\sigma}$ (respectively $\sigma^\dagger$). So, there exists $\epsilon > 0$ such that $g(\sigma_1^\dagger + \epsilon)$ and $g(\hat{\sigma}_1 - \epsilon)$ are well defined and are strictly inside the set B by the alternating signs assumption. Note also that since the set C is closed, if it is made of disjoint closed intervals inside B, then we can apply the implicit function theorem to the end points of these intervals to extend g. So, there exists a continuously differentiable function $g\colon I \to B$.

Now consider $h\colon I \to (\mathbb{R}_{>0})^{n-1}$ defined by $h(\sigma_1) = \lambda_n(\sigma_1, g(\sigma_1))$. We aim to show that $h'(\sigma_1) \neq 0$ for all $\sigma_1 \in I$ which would lead to a contradiction by Rolle's theorem since we know that $h(\sigma_1^\dagger) = h(\hat{\sigma}_1) = \lambda_n(\sigma^\dagger)$. Indeed,

$$h'(\sigma_1) = \partial_1 \lambda_n + \langle (\partial_i \lambda_n)_{i=2}^n, g'(\sigma_1) \rangle = \partial_1 \lambda_n - \langle (\partial_i \lambda_n)_{i=2}^n, (\Lambda'_{[n-1]})^{-1} (\partial_1 \lambda_j)_{j=1}^{n-1} \rangle = \frac{\det(\Lambda'(\sigma))}{\det(\Lambda'_{[n-1]}(\sigma))},$$

where the final equality is due to the determinant formula for block matrices. Since $\Lambda'(\sigma)$ is invertible, we must have $h'(\sigma_1) \neq 0$ for all $\sigma_1 \in I$. □

Remark 3.5. We mention here that if condition (i) was relaxed to $\Lambda'(\sigma)$ is invertible for every $n \geq 2$ and every $\sigma \in B \overset{\text{def.}}{=} [a, b]^n$ for some $0 < a < b$ and $\sigma^\dagger$ is in the interior of B, then our proof implies that the least squares objective f has only one critical point in the interior of B. As we discuss in the following section, in practice, we observe numerically that the Jacobian $\Lambda'(\sigma)$ has non-zero determinant for every $\sigma \in (\mathbb{R}_{>0})^n$.

3.2.2 Discussion on the assumptions

Now, we go back to the two conditions under which the result of Proposition 3.4 holds.

Condition (i). We first rigorously prove that this condition is satisfied in the case where $\sigma = \mathbf{1}$. The proof makes use of the fact that, in this case, we only need to deal with harmonic functions, whose explicit expression is simple.

Lemma 3.6 *If $\sigma = \mathbf{1}$ and $m = n$ then*

$$(-1)^{\frac{n(n+1)}{2}} \det \Lambda'(\sigma) > 0 \quad \textit{and} \quad (-1)^{\frac{n(n-1)}{2}} \det \Lambda'_{[n-1]}(\sigma) > 0. \tag{9}$$

Proof. Since $\sigma = \mathbf{1}$, we have that $u_j(r, \theta) = j^{-1} r^j \cos(j\theta)$ (see Section 2.1), so that $\|\nabla u_j(r, \theta)\|_2^2 = r^{2(j-1)}$, for $j = 1, \dots, n$. Thus, by (4), we have

$$\partial_i \lambda_j(\sigma) = -\frac{1}{\pi} \int_{r_i}^{r_{i-1}} \int_0^{2\pi} \|\nabla u_j(r, \theta)\|_2^2 r \, d\theta dr = -j^{-1}(r_{i-1}^{2j} - r_i^{2j}).$$

Number of annuli n	2	3	4	5	6
Order of min. of $(-1)^{n(n+1)/2}\det\Lambda'(\sigma)$	10^{-2}	10^{-4}	10^{-7}	10^{-11}	10^{-15}
Order of min. of $(-1)^{n(n-1)/2}\det\Lambda'_{[n-1]}(\sigma)$	10^{-1}	10^{-2}	10^{-4}	10^{-7}	10^{-11}
Order of min. of $\min_{1\le k\le n}(-1)^{n(n-1)/2}\det M_k(\sigma)$	10^{-1}	10^{-3}	10^{-6}	10^{-9}	10^{-13}
Order of min. of $\sigma_{\min}(\Lambda'(\sigma))$	10^{-2}	10^{-3}	10^{-4}	10^{-5}	10^{-6}
Order of min. of $\sigma_{\min}(\Lambda'_{[n-1]}(\sigma))$	10^{-1}	10^{-2}	10^{-3}	10^{-4}	10^{-5}

Table 1: order of the minimum value of $(-1)^{n(n+1)/2}\det\Lambda'(\sigma)$, $(-1)^{n(n-1)/2}\det\Lambda'_{[n-1]}(\sigma)$, $\min_{1\le k\le n}(-1)^{n(n-1)/2}\det M_k(\sigma)$, $\sigma_{\min}(\Lambda'(\sigma))$ and $\sigma_{\min}(\Lambda'_{[n-1]}(\sigma))$ over a discretization of $[a,b]^n$ as a function of n, with $m=n$ and $(a,b)=(0.5,1.5)$.

Let $A_i\in\mathbb{R}^n$ be the column vector given by $(A_i)_j=R_i^j$, where $R_i=r_i^2$. Note that $A_n=0$. Then, using that the determinant is a multilinear function, we obtain

$$\det\Lambda'(\sigma)=\frac{(-1)^n}{n!}\det[A_0-A_1,A_1-A_2,\dots,A_{n-2}-A_{n-1},A_{n-1}]=\frac{(-1)^n}{n!}\det[A_0,A_1,\dots,A_{n-2},A_{n-1}].$$

Therefore

$$\det\Lambda'(\sigma)=\frac{(-1)^n}{n!}\det\begin{bmatrix}R_0 & R_1 & \cdots & R_{n-1}\\ R_0^2 & R_1^2 & \cdots & R_{n-1}^2\\ \vdots & \vdots & \dots & \vdots\\ R_0^n & R_1^n & \cdots & R_{n-1}^n\end{bmatrix}=\frac{(-1)^n}{n!}\left(\prod_{i=1}^{n-1}R_i\right)\det\begin{bmatrix}1 & 1 & \cdots & 1\\ R_0 & R_1 & \cdots & R_{n-1}\\ \vdots & \vdots & \dots & \vdots\\ R_0^{n-1} & R_1^{n-1} & \cdots & R_{n-1}^{n-1}\end{bmatrix}.$$

The latter is a Vandermonde matrix, for which the determinant can be explicitly computed. More precisely, we have

$$\det\Lambda'(\sigma)=\frac{(-1)^n}{n!}\left(\prod_{i=1}^{n-1}R_i\right)\prod_{0\le i<j\le n-1}(R_j-R_i)=(-1)^{n+\frac{n(n-1)}{2}}\frac{1}{n!}\left(\prod_{i=1}^{n-1}R_i\right)\prod_{0\le i<j\le n-1}(R_i-R_j).$$

This concludes the proof of the result concerning the sign of $\det\Lambda'(\sigma)$, since $R_i>R_j$ for $i<j$.

Concerning the sign of $\det\Lambda'_{[n-1]}(\sigma)$, we stress that removing the row corresponding to the outermost annulus corresponds to removing the column A_0-A_1 in the computation above. As a result, the same argument applies. □

Unfortunately, we have been unable to prove this rigorously in the general case. This may require studying the dependence of the integrals of $\|\nabla u_j\|_2^2$ on j and on the radii of the subdomains quantitatively, see Garofalo and Lin (1986); Di Cristo and Rondi (2021). As stated in Section 2.2, we always observe numerically that (9) holds, regardless of the value of n and of σ. In Table 1, we show the minimum value of $(-1)^{n(n+1)/2}\det\Lambda'(\sigma)$, $(-1)^{n(n-1)/2}\det\Lambda'_{[n-1]}(\sigma)$, $\sigma_{\min}(\Lambda'(\sigma))$ (the smallest singular value of $\Lambda'(\sigma)$) and $\sigma_{\min}(\Lambda'_{[n-1]}(\sigma))$ over I_k^n, where $I_k=\{a+(i/(k-1))(b-a):0\le i\le k-1\}$ with $k=5$ and $(a,b)=(0.5,1.5)$. The minimum of $(-1)^{n(n+1)/2}\det\Lambda'(\sigma)$ seems to be reached at $b\mathbf{1}$, so that increasing b would result in an even smaller value for the minimum.

Condition (ii). The alternating signs condition can be shown to hold *locally* under a slightly stronger Jacobian invertibility assumption, which we also verified numerically for small values of n (see Table 1): *for every $n\ge1$, every $\sigma\in(\mathbb{R}_{>0})^n$ and every $k\in\{1,\dots,n\}$, $\det(M_k(\sigma))$ has constant sign (independent of k and σ), where $M_k(\sigma)\in\mathbb{R}^{(n-1)\times(n-1)}$ is obtained by removing the last row and the k-th column of $\Lambda'(\sigma)$.*

As in the proof of Proposition 3.4, by the implicit function theorem, there exists a C^1 function g around $\sigma_1^\dagger$ taking values in $(\mathbb{R}_{>0})^{n-1}$ such that

$$\forall j = 1, \dots, n-1, \quad \lambda_j(\sigma_1, g(\sigma_1)) = \lambda_j(\sigma^\dagger).$$

Moreover, locally around $\sigma^\dagger$, its derivative satisfies (8). By Cramer's rule, $g'(\sigma_1)_k = -\det(A_k)/\det(\Lambda'_{[n-1]})$ where A_k is $\Lambda'_{[n-1]}$ with its k-th column replaced by $(\partial_1 \lambda_j)_{j=1}^{n-1}$. By assumption, $\det(A_1)$ and $\det(\Lambda'_{[n-1]})$ have the same sign; $\det(A_2)$ and $\det(\Lambda'_{[n-1]})$ have opposite signs (since we need to swap the first and second columns of A_2 to have the columns and rows correspond to increasing annulus position and increasing measurement frequency). Likewise, $\det(A_3)$ and $\det(\Lambda'_{[n-1]})$ have the same signs (two column swaps needed) and so on. As a result, we obtain that $\operatorname{sign}(g'_k(\sigma_1)) = (-1)^k$.

4 A convex programming approach

In the last decades, various convexification strategies have been proposed Klibanov et al. (2017, 2019). More recently, Harrach (2023) showed that the Calderón problem can be formulated as a convex nonlinear semidefinite program (SDP). To our knowledge, this is the first convex reformulation that is valid in the finite measurements and noisy setting. Given our finding that the least-squares objective has no spurious critical points, it is natural to compare the performance of the two approaches. As pointed out in Section 1.2, the method introduced in Harrach (2023) has not been implemented numerically, as the main result of this work is not constructive and how to find the minimal number of measurements and the parameters defining the convex program is not discussed. In this section, focusing on the case of radial piecewise constant conductivities, we propose a way to estimate these parameters and to solve the convex nonlinear SDP.

4.1 Description of the approach

Given an unknown conductivity $\sigma^\dagger$ and a priori bounds $a, b \in \mathbb{R}_{>0}$ such that $a < b$ and $\sigma^\dagger \in [a, b]^n$, it was proposed in Harrach (2023) to recover $\sigma^\dagger$ by solving the following problem

$$\min_{\sigma \in [a,b]^n} \langle c, \sigma \rangle \quad \text{s.t.} \quad \Lambda(\sigma) \leq y, \tag{$\mathcal{P}_c(y)$}$$

where $c \in (\mathbb{R}_{>0})^n$ is a suitably chosen weight vector and $y = \Lambda(\sigma^\dagger)$. Owing to the convexity of Λ, problem ($\mathcal{P}_c(y)$) is *convex*. This is particularly appealing, as the nonlinearity of the forward map typically leads to the resolution of non-convex optimization problems (such as nonlinear least squares), which are in principle considerably harder to solve.

The main contribution of Harrach (2023) is to show that, if m is sufficiently large, there *exists* a vector $c \in (\mathbb{R}_{>0})^n$ such that, for every unknown conductivity $\sigma^\dagger \in [a, b]^n$, problem ($\mathcal{P}_c(y)$) with $y = \Lambda(\sigma^\dagger)$ has a unique solution, which is $\sigma^\dagger$ (see Theorem 3.2 in the above reference). In the following, we say that such a vector c is *universal*. The main issue with this result is that its proof is not constructive, and hence, c is unknown in practice.

4.2 Numerical implementation

We now present a numerical procedure to estimate a universal vector c, which can then be used to investigate the properties of ($\mathcal{P}_c(y)$) for practical purposes. We first discuss an equivalent characterization of universality of the weight vector c by first order optimality conditions and will exploit this characterization.

Optimality conditions. Since problem ($\mathcal{P}_c(y)$) is convex, it is natural to investigate whether strong duality holds (we refer the reader to Boyd and Vandenberghe (2004, Section 5) for more details on strong duality, constraint qualification and optimality conditions). If $y = \Lambda(b\mathbf{1})$, then ($\mathcal{P}_c(y)$) has a unique admissible point, which is $b\mathbf{1}$. Otherwise, one can show that Slater's condition holds, which implies that strong duality holds. As a result, we obtain the following necessary and sufficient first-order optimality conditions.

Lemma 4.1 *Let $\sigma \in [a,b]^n$ and $y \in \mathbb{R}^m$ be such that $y_j > \lambda_j(b\mathbf{1})$ for every $1 \le j \le m$. Then σ is a solution to ($\mathcal{P}_c(y)$) if and only if there exists $z \in \mathbb{R}^m$ and $\lambda, \mu \in \mathbb{R}^n$ such that*

$$\begin{cases} \lambda, \mu \ge 0 \text{ and } z \ge 0, \\ \lambda_i(\sigma_i - a) = 0 \text{ and } \mu_i(\sigma_i - b) = 0 \text{ for every } 1 \le i \le n, \\ z_j(\lambda_j(\sigma) - y_j) = 0 \text{ for every } 1 \le j \le m, \\ c + \mu - \lambda + \sum_{j=1}^m z_j \nabla \lambda_j(\sigma) = 0. \end{cases} \tag{10}$$

Proof. Since Λ is continuous, there exists $\delta > 0$ such that, for every $\sigma \in (\mathbb{R}_{>0})^n$ with $\|\sigma - b\mathbf{1}\|_\infty \le \delta$, it holds

$$\lambda_j(\sigma) - \lambda_j(b\mathbf{1}) \le [y_j - \lambda_j(b\mathbf{1})]/2, \qquad 1 \le j \le m.$$

Taking $\sigma = (b-\delta)\mathbf{1}$, we obtain for every $1 \le j \le m$ that

$$\begin{aligned} y_j - \lambda_j(\sigma) &= y_j - \lambda_j(b\mathbf{1}) + \lambda_j(b\mathbf{1}) - \lambda_j(\sigma) \\ &\ge (y_j - \lambda_j(b\mathbf{1}))/2 \\ &> 0. \end{aligned}$$

As a result, we have proved the existence of $\sigma \in (a,b)^n$ such that $\lambda_j(\sigma) < y_j$ for every $1 \le j \le m$, which shows that Slater's condition holds. The necessary and sufficient optimality condition then follows from the convexity of Λ. □

4.2.1 Estimation of the weight vector

We propose to estimate c by exploiting the optimality conditions (10). To be more precise, we fix n_σ a set of conductivities $\{\sigma_l\}_{1 \le l \le n_\sigma} \subset [a,b]^n$ and try to find a vector c such that σ_l is a solution to ($\mathcal{P}_c(y)$) with $y = \Lambda(\sigma_l)$ for every $1 \le l \le n_\sigma$. By Proposition 4.1, this is equivalent to the existence, for every $1 \le l \le n_\sigma$, of $(\lambda_l, \mu_l, z_l) \in \mathbb{R}^n \times \mathbb{R}^n \times \mathbb{R}^m$ such that (10) holds. The crucial point is that this constraint is *linear* in c. As a result, given the problem parameters (n, m, a, b) and $\{\sigma_l\}_{1 \le l \le n_\sigma} \subset [a,b]^n$, one can check that c is such that every σ_l is a solution to ($\mathcal{P}_c(y)$) with $y = \Lambda(\sigma_l)$ by solving a *linear feasibility problem*, for which efficient solvers exist. If this holds and $\{\sigma_l\}_{1 \le l \le n_\sigma}$ is a sufficiently fine discretization of $[a,b]^n$, one can moreover hope that the estimated c is universal. The resulting linear feasibility problem reads as follows:

$$\begin{aligned} \max_{\substack{c \in \mathbb{R}^n \\ \lambda, \mu \in \mathbb{R}^{n_\sigma \times n} \\ z \in \mathbb{R}^{n_\sigma \times m}}} \quad & c_n \\ \text{s.t.} \quad & c \ge 0 \text{ and } c_1 = 1, \\ & \lambda, \mu \ge 0 \text{ and } z \ge 0, \\ & \lambda_{l,i}(\sigma_{l,i} - a) = 0 \text{ and } \mu_{l,i}(\sigma_{l,i} - b) = 0, \quad 1 \le i \le n, 1 \le j \le n_\sigma, \\ & c_i + \mu_{l,i} - \lambda_{l,i} + \sum_{j=1}^m z_{l,j} \partial_i \lambda_j(\sigma_l) = 0, \qquad 1 \le i \le n,\ 1 \le l \le n_\sigma. \end{aligned} \tag{11}$$

The constraint $c_1 = 1$ allows us to circumvent the fact that solutions of ($\mathcal{P}_c(y)$) are unchanged by the multiplication of c by a positive constant. The maximization of c_n is optional (that is to say, one can simply find a feasible tuple (c, λ, μ, z)). Maximizing c_n allows to ensure that, if $\hat{c}$ is a solution to (11), then any universal vector c must satisfy $c_n \le \hat{c}_n$, as the constraints of (11) is a subset of the constraints that any universal weight vector must satisfy. As a result, maximizing c_n gives us an upper bound on the last coordinate of any universal weight vector.

Number of annuli n	2	3	4	5
Min. num. of measurements m	3	7	13	20
Smallest coefficient of c	$7.8 \cdot 10^{-2}$	$1.5 \cdot 10^{-3}$	$3.6 \cdot 10^{-6}$	$1.1 \cdot 10^{-10}$

Table 2: minimal number of measurements required for the existence of the vector c and smallest coefficient of c as a function of the number of annuli n ($a = 0.5$ and $b = 1.5$).

Number of annuli n	2	3	4	5	6
Min. num. of measurements m	2	5	8	13	19
Smallest coefficient of c	$1.8 \cdot 10^{-1}$	$2.1 \cdot 10^{-2}$	$3.3 \cdot 10^{-4}$	$1.9 \cdot 10^{-6}$	$2.8 \cdot 10^{-9}$

Table 3: minimal number of measurements required for the existence of the vector c and smallest coefficient of c as a function of the number of annuli n ($a = 0.75$ and $b = 1.25$).

Numerical evaluation. We take $(a, b) = (0.5, 1.5)$ and assess the performance of this estimation procedure as follows. We take $\{\sigma_l\}_{1 \leq l \leq n_\sigma}$ to be $(I_k)^n \setminus \{b\mathbf{1}\}$ where $I_k = \{a + (i/(k-1))(b-a) : 0 \leq i \leq k-1\}$ and $k = 5$. We solve the feasibility problem for increasing values of m starting from $m = n$ until it becomes feasible. We use the package `JuMP.jl` (Lubin et al., 2023) to model the feasibility problem, which allows us to try a large number of solvers seamlessly. The results of this experiment are reported in Table 2. The coefficients of the estimated vectors c are displayed in Figure 6a. The minimal number of measurements seems to grow linearly with n and is significantly greater than n even for small values of n. The smallest value of c (which is always c_n, the value corresponding to the innermost annulus) rapidly decreases with n and becomes very small even for small values of n. This means that the estimation of an unknown conductivity with this SDP approach will necessarily enjoy poor stability, as large variations of σ_n will result in small variations of the objective $\langle c, \sigma \rangle$ of ($\mathcal{P}_c(y)$). This phenomenon illustrates the ill-posedness of the inverse problem, which increases with the distance to the boundary and is not resolved by this convex programming approach. For $n = 6$, all the linear programming solvers we have tried (HiGHS (Huangfu and Hall, 2018), SCS (O'Donoghue et al., 2016), Clarabel (Goulart and Chen, 2024), Gurobi, MOSEK) struggled to solve the problem. This could be due to the fact that c_n must be close to machine precision for $n = 6$. Let us stress that our approach for estimating c is also limited by its computational cost. As an example, the linear program we would need to solve for $(n, m, k) = (7, 27, 5)$ involves more than three million variables with more than one million constraints. The results of this experiment heavily depend on the choice of the a piori bounds a and b on the unknown conductivity. If instead of taking $(a, b) = (0.5, 1.5)$ as above we take $(a, b) = (0.75, 1.25)$, the minimal number of measurements is smaller and the smallest coefficient of c is larger. The results in this setting are reported in Table 3 and Figure 6b.

Handcrafting the weight vector. As a final experiment, we investigate the universality of several handcrafted weight vectors c with a decay similar to that of the estimated one. We take $n = 5$, $m = 13$, $(a, b) = (0.75, 1.25)$ and draw 100 random conductivities uniformly in $[a, b]^n$. We solve ($\mathcal{P}_c(y)$) with the estimated vector c and the vector $c = (10^{k_i})_{1 \leq i \leq n}$ with k_i linearly interpolating between $k_1 = 0$ and k_n for several value of k_n (see Figure 7 for a plot of the different choices of c). The histograms of the ℓ^∞ estimation error for the different choices of c are displayed in Figure 8. The first two guesses, which have a faster decay than the estimated c, are approximately universal but yield errors that are slightly larger. On the contrary, the last two guesses, which decay slower than the estimated c, are not universal (they yield errors that are close to that of random guessing on several instances). Still, on the majority of instances, they allow us to obtain an estimation error which is smaller or approximately equal to the one obtained with the estimated c. This suggests that designing the weight vector c by hand instead of relying on the estimation procedure proposed above could be difficult.

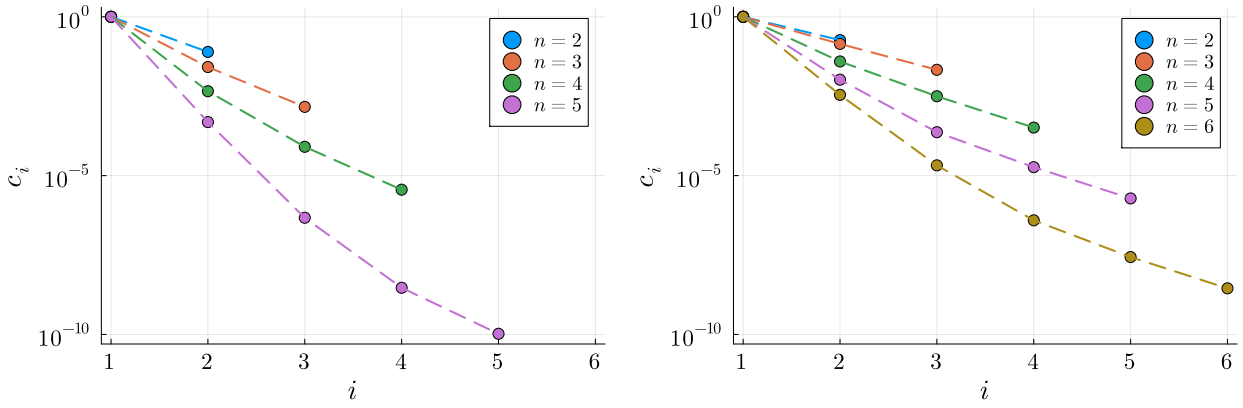

(a) $(a, b) = (0.5, 1.5)$ (b) $(a, b) = (0.75, 1.25)$

Figure 6: coefficients of the estimated vector c in two settings. For each n, the number of measurements m is the one reported in Table 2 (a) or Table 3 (b).

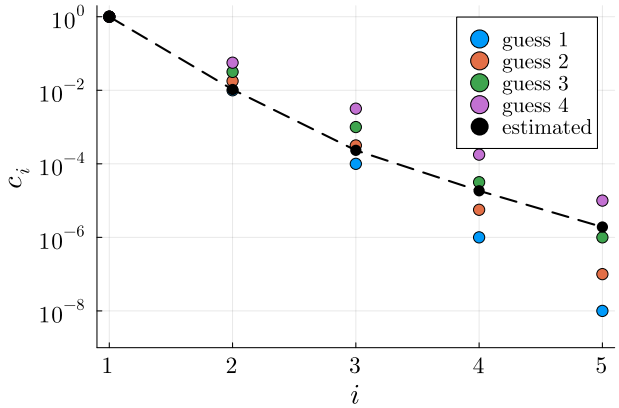

Figure 7: plot of four handcrafted vectors c along with the estimated one for $n = 5$, $m = 13$ and $(a, b) = (0.75, 1.25)$.

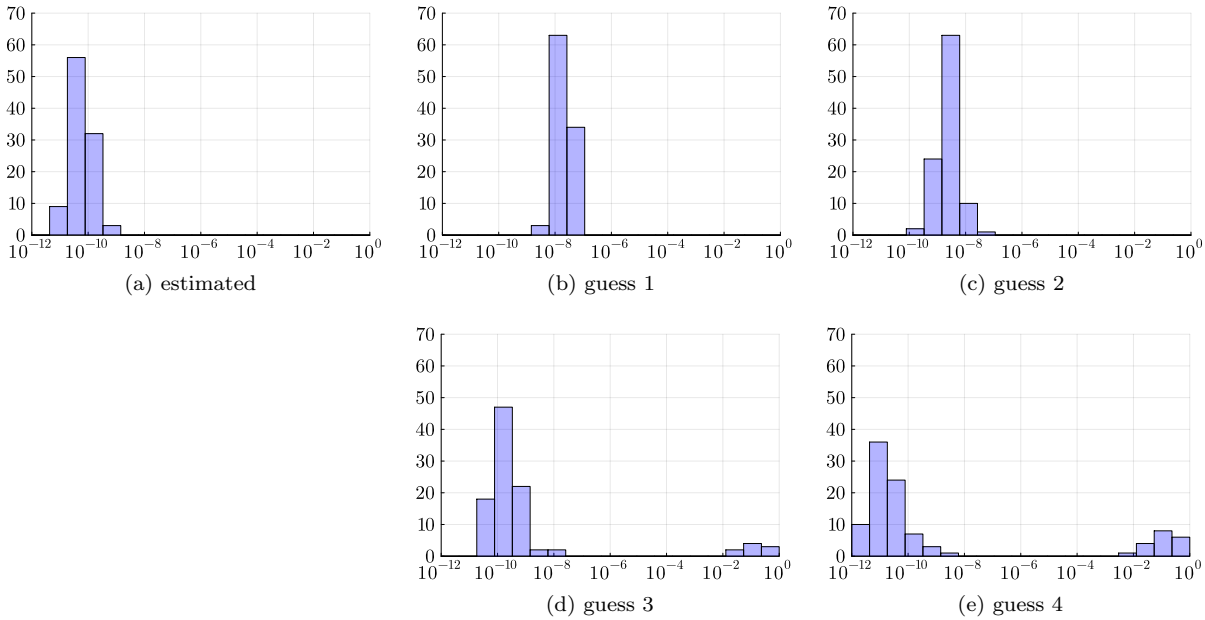

(a) estimated (b) guess 1 (c) guess 2

(d) guess 3 (e) guess 4

Figure 8: histograms of the ℓ^∞ estimation error for $n = 5$, $m = 13$ and $(a, b) = (0.75, 1.25)$ with different choices of c (see Figure 7).

4.2.2 Numerical resolution of the convex nonlinear semidefinite program

Using the proposed procedure to estimate a universal weight vector c, the resolution of the convex nonlinear semidefinite problem ($\mathcal{P}_c(y)$) can be carried out using standard optimization solvers. Since the first and second order derivatives of the forward map Λ can be efficiently computed via automatic differentiation, we propose to solve ($\mathcal{P}_c(y)$) by relying on interior point methods. These algorithms consist in solving ($\mathcal{P}_c(y)$) by applying Newton's method to a sequence of equality constrained problems. We refer the reader to Boyd and Vandenberghe (2004, Chapter 11) for more details on this family of algorithms. In practice, we use the package `Optimization.jl`[2] to model ($\mathcal{P}_c(y)$) and solve it with the Ipopt solver (Wächter and Biegler, 2006).

5 Numerical comparison of several reconstruction methods

In this section, we perform a comparison of various reconstruction methods, both in the case of noiseless and noisy measurements.

5.1 Comparison of the convex approach with least squares

In this subsection, we compare the convex nonlinear SDP approach of Harrach (2023) to the classical least squares approach. In agreement with the results of Section 3, we find that the latter does not suffer from the problem of local convergence, and that, in addition to requiring less measurements and being faster, it always outperforms the convex nonlinear SDP approach. In what follows, we use Powell's dog leg method to solve the least squares problem. This trust-region method combines the steepest and the Gauss-Newton descent directions, and performed best among all the solvers we tested.

[2] https://github.com/SciML/Optimization.jl

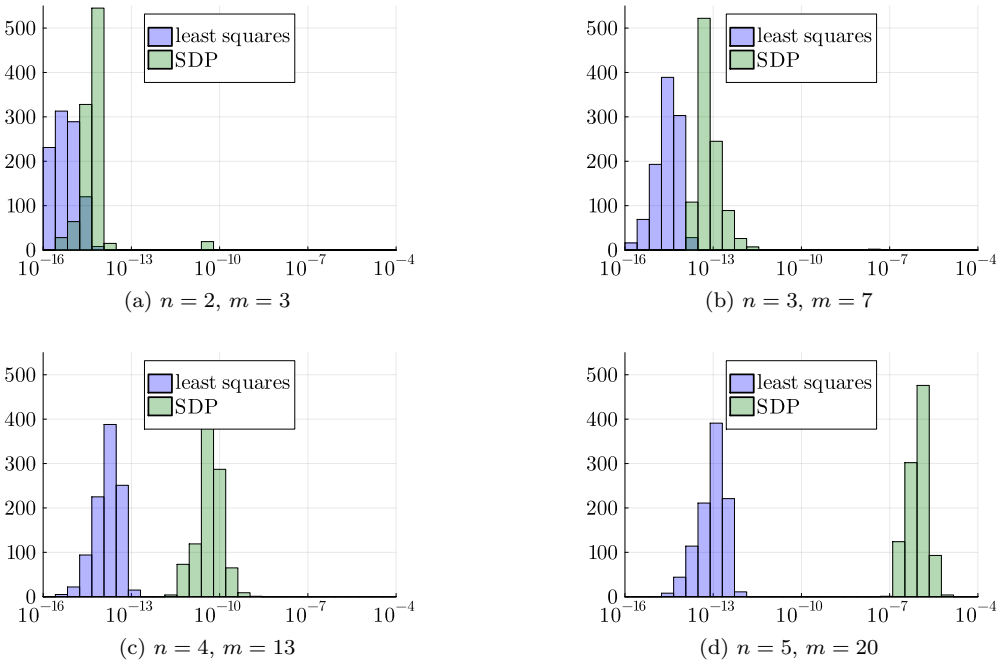

(a) $n = 2$, $m = 3$ (b) $n = 3$, $m = 7$

(c) $n = 4$, $m = 13$ (d) $n = 5$, $m = 20$

Figure 9: histograms of the ℓ^∞ estimation error of the least squares and the SDP approaches on 1000 instances with $(a, b) = (0.5, 1.5)$.

Noiseless setting. To assess this, we take $(a, b) = (0.5, 1.5)$ and $n \in \{2, 3, 4, 5\}$. For each value of n we take m to be the value reported in Table 2. Then, we draw 1000 unknown conductivities $\sigma^\dagger$ uniformly at random in $[a, b]^n$. On each instance, we compare two methods for estimating $\sigma^\dagger$:

1. using the least squares solver initialized uniformly at random in $[a, b]^n$ to find an approximate solution of $\Lambda(\sigma) = \Lambda(\sigma^\dagger)$;
2. solving ($\mathcal{P}_c(y)$) with an interior point method with $y = \Lambda(\sigma^\dagger)$ and c estimated as in Section 4.2.1.

The results of this experiment are displayed in Figure 9. We notice that the least squares approach consistently outperforms the SDP approach. The performance of the latter degrades much faster than the performance of the former as n grows. We also stress that the least squares approach is still able to accurately recover the unknown if m is taken to be equal to n instead of 3 ($n = 2$), 7 ($n = 3$), 13 ($n = 4$) or 20 ($n = 5$). Finally, the least squares approach is significantly faster than the SDP approach, especially for larger values of n.

Noisy setting. We also conduct a similar experiment in the noisy setting, where we only have access to noisy measurements $z = \Lambda(\sigma^\dagger) + w$, where $w \in \mathbb{R}^m$ is an additive noise. In this case, Harrach (2023) proposes to solve ($\mathcal{P}_c(y)$) with $y = z + \delta\mathbf{1}$, where $\delta > 0$ is an estimate of the noise level. We compare this method to the approach that consists in using the least squares solver initialized uniformly at random in $[a, b]^n$ to minimize $\sigma \mapsto \|\Lambda(\sigma) - z\|_2^2$. The experimental setting is the same as above, the coordinates of the noise being independent and uniformly distributed in $(-\delta, \delta)$ with $\delta = 10^{-4}$. The results are reported in Figure 10. The difference of the estimation errors is smaller than in the noiseless setting, but the least squares approach still consistently outperforms the SDP approach.

Influence of the box size. One could argue that enlarging the box size could result in more failures of the least squares approach, as it could suffer from the problem of local convergence. This does not seem to be

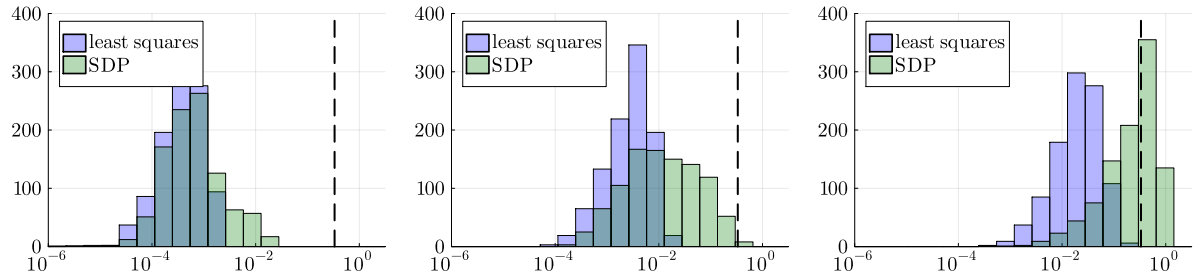

(a) $n = 2$, $m = 3$ (b) $n = 3$, $m = 7$ (c) $n = 4$, $m = 13$

Figure 10: histograms of the ℓ^∞ estimation error of least squares and the SDP approach in the noisy case on 1000 instances with $(a, b) = (0.5, 1.5)$. The dashed black line indicates the mean estimation error of a naive random guessing strategy, which is $(b - a)/3$.

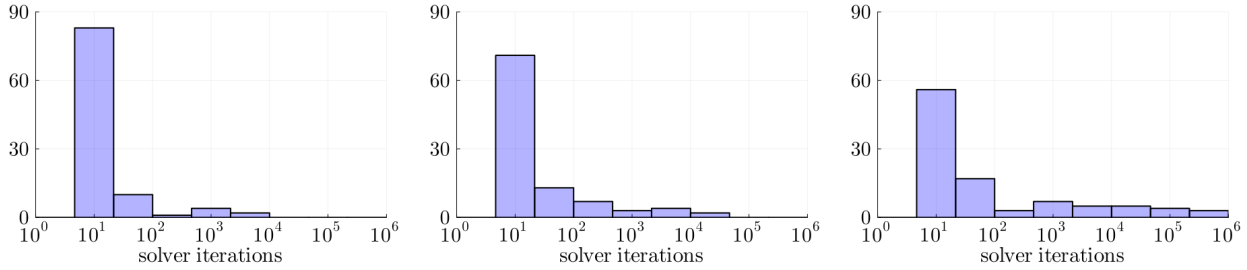

(a) $n = 8$ (b) $n = 9$ (c) $n = 10$

Figure 11: histograms of the number of solver iterations for $n \in \{8, 9, 10\}$. As n increases, the number of instances for which the solver runs for a large number of iterations increases. Still, in most cases, a solution is found in about ten iterations.

the case. When the box is enlarged (for example taking $(a, b) = (0.1, 1.9)$), the performance of the nonlinear SDP approach significantly deterioriates: the minimal number of measurements m significantly increases and the smallest value of c is several orders of magnitude smaller. On the other hand, the performance of the least squares approach is almost unchanged.

Convergence of the least squares solver. When $n \leq 9$, we observed that the least squares solver (Powell's dog leg method) always converges to a global minimum of the least squares objective. When $n \geq 8$, for some worst-case instances, the solver runs for a very large number of iterations, its iterates going far away from the global minimum while keeping a low objective value (the maximum number of iterations over all instances for $n \leq 7$ is 22 and the histograms of the number of iterations for $n \in \{8, 9, 10\}$ are given in Figure 11). After a large number of iterations, the iterates finally converge to the true conductivity. This behavior is showcased in Figure 12 for a specific instance with $n = m = 9$. When $n = 10$, the solver fails to converge on very few instances (of the order of 1 out of 100), after running for several million iterations. The gradient of the objective at the last iterate is non-zero, but its coordinate corresponding to the innermost conductivity is close to machine precision. Our experiments suggest that allowing for more iterations would lead to convergence. Moreover, this phenomenon is likely caused by the ill-posedness of the inverse problem, which allows conductivities that differ by several orders of magnitude to yield measurements that are close. We also stress that convergence failures are never caused by the existence of spurious critical points. Finally, let us recall that, for $n \geq 6$, the SDP approach becomes infeasible, since the the smallest coordinate of c rapidly reaches machine precision as n increases.

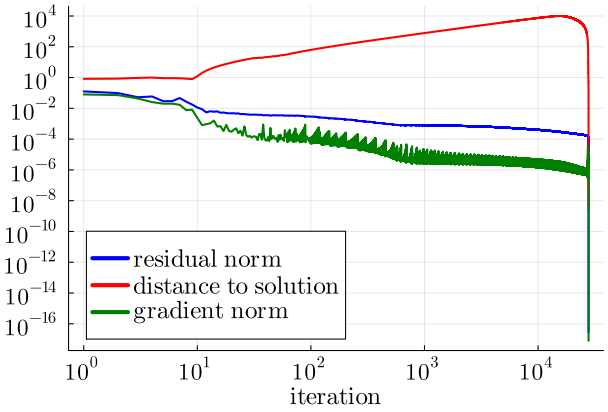

Figure 12: convergence of the least squares solver (Powell's dog leg method) after a large number of iterations for an instance with $n = m = 9$. The iterates reach a maximum distance to the unknown of 10^4 while keeping a small value for the residual $\|\Lambda(\sigma) - \Lambda(\sigma^\dagger)\|_\infty$ (of the order of 10^{-4}). Eventually, we reach a regime where the iterates quickly converge towards the true solution.

5.2 Comparison of least squares and Tikhonov regularization

In this subsection, we investigate the impact of adding a squared ℓ^2 norm penalization to the least squares objective (Tikhonov regularization). Namely, we solve

$$\min_{\sigma \in [a,b]^n} \|\Lambda(\sigma) - y\|_2^2 + \lambda \|\sigma - [(a+b)/2]\mathbf{1}\|_2^2 \qquad (\mathcal{Q}_\lambda(y))$$

for several values of λ. We stress that $(\mathcal{Q}_\lambda(y))$ is a non-convex optimization problem who could have spurious local minima. We are mainly interested in understanding whether the introduction of the regularization term could introduce additional spurious local minima.

We draw a large number of random unknown conductivities $\sigma^\dagger$ uniformly in $[a,b]^n$. Then, for each unknown conductivity, we draw a random guess uniformly in $[a,b]^n$ and run a trust-region algorithm initialized with this guess on $(\mathcal{Q}_\lambda(y))$ for several values of λ. The least squares estimate $\hat{\sigma}_{\mathrm{ls}}$ is defined as the estimated conducitivity obtained for $\lambda = 0$ and the Tikhonov estimate $\hat{\sigma}_{\mathrm{tk}}$ as the estimated conductivity yielding the smallest ℓ^∞ estimation error among all tested positive values of λ.[3]

We take $n = 3$ and $m = 5$, as well as $(a,b) = (0.5, 1.5)$. The number of unknown conductivities is 100 and the noise is a centered Gaussian with standard deviation 10^{-3}. We consider values of λ in the set $(10^{\alpha_i})_{1 \le i \le 20}$ with $(\alpha_i)_{1 \le i \le 20}$ a uniform discretization of $(-7, -2)$. The results of this experiment are displayed in Figure 13. We notice that, on average, Tikhonov regularization yields a lower estimation error than least squares. Yet, for about half the instances, least squares performs slightly better and the optimal λ is the smallest tested value (which is 10^{-7}). Athough the addition of the squared ℓ^2 norm term could in principle add new spurious local minima to the objective, we still observe that it is on average beneficial.

If the unknowns are small perturbations of the constant conductivity $[(a+b)/2]\mathbf{1}$, then Tikhonov regularization is even more beneficial. This is evidenced in Figure 14, which displays the results of the same experiment as above, but with the unknowns being drawn uniformly at random in $[(a+b)/2 - \epsilon, (a+b)/2 + \epsilon]$ with $\epsilon = (b-a)/20$.

[3] This scenario favors Tikhonov regularization as the true ℓ^∞ estimation error would not be available in a practical scenario, making the choice of λ more difficult.

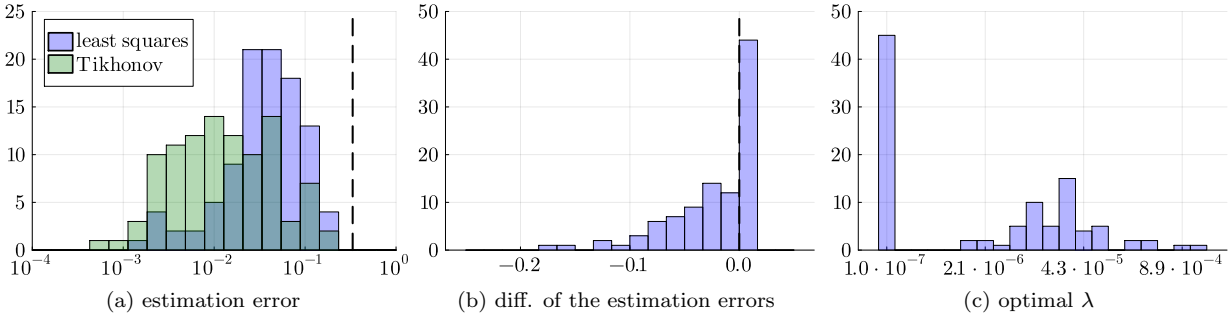

(a) estimation error (b) diff. of the estimation errors (c) optimal λ

Figure 13: histograms of the estimation error $\|\hat{\sigma} - \sigma^\dagger\|_\infty$, of the difference $\|\hat{\sigma}_{\mathrm{tk}} - \sigma^\dagger\|_\infty - \|\hat{\sigma}_{\mathrm{ls}} - \sigma^\dagger\|_\infty$ of the Tikhonov estimation error and the least squares estimation error, and of the value of λ yielding the smallest estimation error ($n = 3$, $m = 5$ and $(a, b) = (0.5, 1.5)$). The dashed black line in (a) corresponds to the average estimation error of a random guess (that is $(b - a)/3$).

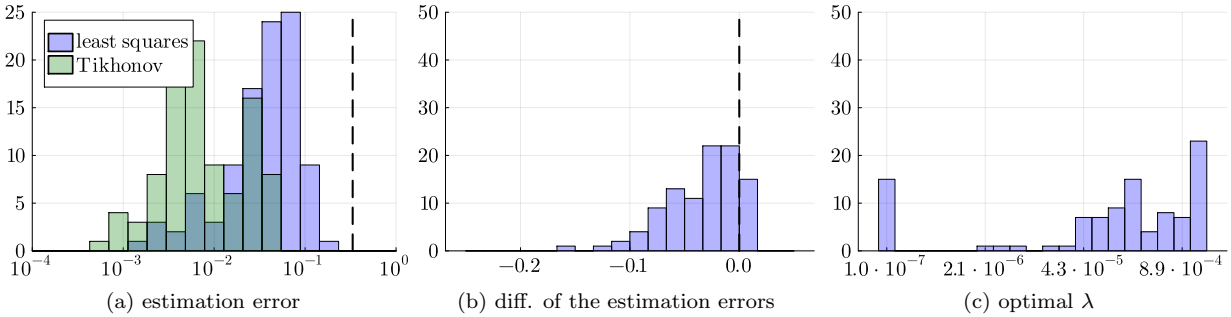

(a) estimation error (b) diff. of the estimation errors (c) optimal λ

Figure 14: same as Figure 13, with unknowns being small perturbations of the constant conductivitiy $[(a + b)/2]\mathbf{1}$.

6 Conclusion

We carried out an extensive numerical investigation of the least squares approach in the context of the piecewise constant radial Calderón problem. Contrary to previous claims, this approach does not seem to suffer from the presence of spurious local minimums and we observed a good convergence behavior even in the presence of noise. Furthermore, we observed numerically that the Jacobian of the forward map has always full rank. Under this assumption and an additional monotonicity condition (both rigorously verified in the case of $n = 2$ unknowns) we have proved that exact recovery is achieved whenever the number of measurements m is at least the number of unknowns n. Under the same assumptions, we have showed that, when $m = n$, all critical points of the least squares objective are global minimums.

Our results suggest that the optimization landscape of the least squares objective warrants further investigations. An interesting and challenging future direction is the study of this landscape in the noisy regularized setting. The codebase we developed might also serve as a useful benchmark for further studies on this topic.

Acknowledgments

G.S.A. is supported by the Air Force Office of Scientific Research under award number FA8655-23-1-7083 and by the European Union (ERC, SAMPDE, 101041040). Views and opinions expressed are however those of the authors only and do not necessarily reflect those of the European Union or the European Research Council. Neither the European Union nor the granting authority can be held responsible for them. G.S.A. is a member of the "Gruppo Nazionale per l'Analisi Matematica, la Probabilità e le loro Applicazioni", of the "Istituto Nazionale di Alta Matematica". The research was supported in part by the MIUR Excellence Department Project awarded to Dipartimento di Matematica, Università di Genova, CUP D33C23001110001. Co-funded by European Union – Next Generation EU, Missione 4 Componente 1 CUP D53D23005770006 and CUP D53D23016180001. The work of R.P. was supported by the European Union (ERC, SAMPDE, 101041040 and ERC, WOLF, 101141361). G.S.A. and C.P. acknowledge support from a Royal Society International Exchanges award.

References

Alberti, G. S., Petit, R., and Sanna, S. (2025). A convex lifting approach for the Calderón problem. *arXiv preprint arXiv:2507.00645*.

Alberti, G. S. and Santacesaria, M. (2019). Calderón's inverse problem with a finite number of measurements. *Forum of Mathematics, Sigma*, 7:e35.

Alberti, G. S. and Santacesaria, M. (2022). Infinite-Dimensional Inverse Problems with Finite Measurements. *Archive for Rational Mechanics and Analysis*, 243(1):1–31.

Alessandrini, G. (1988). Stable determination of conductivity by boundary measurements. *Applicable Analysis*, 27(1-3):153–172.

Alessandrini, G. (2012). Strong unique continuation for general elliptic equations in 2D. *Journal of Mathematical Analysis and Applications*, 386(2):669–676.

Alessandrini, G. and Scapin, A. (2017). Depth dependent resolution in electrical impedance tomography. *J. Inverse Ill-Posed Probl.*, 25(3):391–402.

Alessandrini, G. and Vessella, S. (2005). Lipschitz stability for the inverse conductivity problem. *Advances in Applied Mathematics*, 35(2):207–241.

Astala, K. and Päivärinta, L. (2006). Calderón's inverse conductivity problem in the plane. *Annals of Mathematics*, pages 265–299.

Bacchelli, V. and Vessella, S. (2006). Lipschitz stability for a stationary 2D inverse problem with unknown polygonal boundary. *Inverse Problems*, 22(5):1627.

Barceló, J. A., Castro, C., Macià, F., and Meroño, C. J. (Thu Feb 01 05:00:00 UTC 2024). The Born approximation in the three-dimensional Calderón problem ii: Numerical reconstruction in the radial case. *Inverse Problems and Imaging*, 18(1):183–207.

Beretta, E., de Hoop, M. V., and Qiu, L. (2013). Lipschitz Stability of an Inverse Boundary Value Problem for a Schrödinger-Type Equation. *SIAM Journal on Mathematical Analysis*, 45(2):679–699.

Beretta, E. and Francini, E. (2022). Global Lipschitz stability estimates for polygonal conductivity inclusions from boundary measurements. *Applicable Analysis*, 101(10):3536–3549.

Bezanson, J., Edelman, A., Karpinski, S., and Shah, V. B. (2017). Julia: A Fresh Approach to Numerical Computing. *SIAM Review*, 59(1):65–98.

Boyd, S. and Vandenberghe, L. (2004). *Convex Optimization*. Cambridge University Press, Cambridge New York Melbourne New Delhi Singapore, 1st edition edition.

Brojatsch, A. and Harrach, B. (2024). On the required number of electrodes for uniqueness and convex reformulation in an inverse coefficient problem. *arXiv preprint arXiv:2411.00482*.

Bukhgeim, A. L. (2008). Recovering a potential from Cauchy data in the two-dimensional case. *Journal of Inverse and Ill-posed Problems*, 16(1):19–33.

Calderón, A. P. (1980). On an inverse boundary value problem. *Seminar on Numerical Analysis and its Applications to Continuum Physics*, 25:65–73.

Caro, P. and Rogers, K. M. (2016). Global Uniqueness for the Calderón Problem with Lipschitz Conductivities. *Forum of Mathematics, Pi*, 4:e2.

Dalle, G. and Hill, A. (2024). DifferentiationInterface.jl.

Daudé, T., Macià, F., Meroño, C. J., and Nicoleau, F. (2024). Stable factorization of the Calderón problem via the Born approximation.

Di Cristo, M. and Rondi, L. (2021). Interior decay of solutions to elliptic equations with respect to frequencies at the boundary. *Indiana Univ. Math. J.*, 70(4):1303–1334.

Garde, H. (2020). Reconstruction of piecewise constant layered conductivities in electrical impedance tomography. *Comm. Partial Differential Equations*, 45(9):1118–1133.

Garde, H. (2022). Simplified reconstruction of layered materials in EIT. *Appl. Math. Lett.*, 126:Paper No. 107815, 5.

Garde, H. and Hyvönen, N. (2020). Optimal depth-dependent distinguishability bounds for electrical impedance tomography in arbitrary dimension. *SIAM J. Appl. Math.*, 80(1):20–43.

Garde, H. and Knudsen, K. (2017). Distinguishability revisited: depth dependent bounds on reconstruction quality in electrical impedance tomography. *SIAM J. Appl. Math.*, 77(2):697–720.

Garofalo, N. and Lin, F.-H. (1986). Monotonicity properties of variational integrals, A_p weights and unique continuation. *Indiana Univ. Math. J.*, 35(2):245–268.

Goulart, P. J. and Chen, Y. (2024). Clarabel: An interior-point solver for conic programs with quadratic objectives.

Hanke, M., Neubauer, A., and Scherzer, O. (1995). A convergence analysis of the Landweber iteration for nonlinear ill-posed problems. *Numerische Mathematik*, 72(1):21–37.

Harrach, B. (2023). The Calderón Problem with Finitely Many Unknowns is Equivalent to Convex Semidefinite Optimization. *SIAM Journal on Mathematical Analysis*, pages 5666–5684.

Harrach, B. and Meftahi, H. (2025). A monotonicity-based globalization of the level-set method for inclusion detection. *arXiv preprint arXiv:2501.15887*.

Hill, A. and Dalle, G. (2025). Sparser, Better, Faster, Stronger: Efficient Automatic Differentiation for Sparse Jacobians and Hessians.

Huangfu, Q. and Hall, J. A. J. (2018). Parallelizing the dual revised simplex method. *Mathematical Programming Computation*, 10(1):119–142.

Kaltenbacher, B. (2024). Convergence rates under a range invariance condition with application to electrical impedance tomography. *IMA Journal of Numerical Analysis*, page drae063.

Kaltenbacher, B., Neubauer, A., and Scherzer, O. (2008). *Iterative regularization methods for nonlinear ill-posed problems*, volume 6 of *Radon Series on Computational and Applied Mathematics*. Walter de Gruyter GmbH & Co. KG, Berlin.

Kindermann, S. (2022). On the tangential cone condition for electrical impedance tomography. *Electron. Trans. Numer. Anal.*, 57:17–34.

Klibanov, M. V., Kolesov, A. E., Nguyen, L., and Sullivan, A. (2017). Globally strictly convex cost functional for a 1-d inverse medium scattering problem with experimental data. *SIAM Journal on Applied Mathematics*, 77(5):1733–1755.

Klibanov, M. V., Li, J., and Yang, Z. (2025). Convexification with the viscocity term for electrical impedance tomography. *arXiv preprint arXiv:2503.07916*.

Klibanov, M. V., Li, J., and Zhang, W. (2019). Convexification of electrical impedance tomography with restricted Dirichlet-to-Neumann map data. *Inverse Problems*, 35(3):035005.

Knudsen, K., Lassas, M., Mueller, J. L., and Siltanen, S. (2007). D-Bar Method for Electrical Impedance Tomography with Discontinuous Conductivities. *SIAM Journal on Applied Mathematics*, 67(3):893–913.

Lazzaro, D., Morigi, S., and Ratti, L. (2024). Oracle-net for nonlinear compressed sensing in electrical impedance tomography reconstruction problems. *Journal of Scientific Computing*, 101(2):49.

Lechleiter, A. and Rieder, A. (2008). Newton regularizations for impedance tomography: convergence by local injectivity. *Inverse Problems*, 24(6):065009, 18.

Lubin, M., Dowson, O., Dias Garcia, J., Huchette, J., Legat, B., and Vielma, J. P. (2023). JuMP 1.0: Recent improvements to a modeling language for mathematical optimization. *Mathematical Programming Computation*, 15:581–589.

Mandache, N. (2001). Exponential instability in an inverse problem for the Schrödinger equation. *Inverse Problems*, 17(5):1435.

Nachman, A. I. (1996). Global Uniqueness for a Two-Dimensional Inverse Boundary Value Problem. *Annals of Mathematics*, 143(1):71–96.

Neubauer, A. (2000). On Landweber iteration for nonlinear ill-posed problems in Hilbert scales. *Numerische Mathematik*, 85(2):309–328.

O'Donoghue, B., Chu, E., Parikh, N., and Boyd, S. (2016). Conic optimization via operator splitting and homogeneous self-dual embedding. *Journal of Optimization Theory and Applications*, 169(3):1042–1068.

Revels, J., Lubin, M., and Papamarkou, T. (2016). Forward-Mode Automatic Differentiation in Julia.

Rondi, L. (2006). A remark on a paper by G. Alessandrini and S. Vessella: "Lipschitz stability for the inverse conductivity problem" [Adv. in Appl. Math. **35** (2005), no. 2, 207–241; mr2152888]. *Adv. in Appl. Math.*, 36(1):67–69.

Schäfer, F., Tarek, M., White, L., and Rackauckas, C. (2022). Abstractdifferentiation.jl: Backend-agnostic differentiable programming in julia.

Siltanen, S., Mueller, J., and Isaacson, D. (2000). An implementation of the reconstruction algorithm of A Nachman for the 2D inverse conductivity problem. *Inverse Problems*, 16(3):681.

Sylvester, J. (1992). A Convergent Layer Stripping Algorithm for the Radially Symmetric Impedence Tomography Problem. *Communications in Partial Differential Equations*, 17(11-12):1955–1994.

Sylvester, J. and Uhlmann, G. (1987). A Global Uniqueness Theorem for an Inverse Boundary Value Problem. *Annals of Mathematics*, 125(1):153–169.

Wächter, A. and Biegler, L. T. (2006). On the implementation of an interior-point filter line-search algorithm for large-scale nonlinear programming. *Mathematical Programming*, 106(1):25–57.

Winkler, R. and Rieder, A. (2014). Resolution-controlled conductivity discretization in electrical impedance tomography. *SIAM J. Imaging Sci.*, 7(4):2048–2077.